Journal of Biological Chemistry (2010) 285(49): 38674-38683.

Ca^<2+> Release to Lumen from ADP-sensitive Phosphoenzyme E1PCa_2 without Bound K^+ of Sarcoplasmic Reticulum Ca^<2+>-ATPase

Yamasaki, Kazuo ; Daiho, Takashi ; Danko, Stefania ; Suzuki, Hiroshi

Ca^{2+} Release to Lumen from ADP-sensitive Phosphoenzyme $E1PCa_2$ without Bound K^+ of Sarcoplasmic Reticulum Ca^{2+}-ATPase *

Kazuo Yamasaki, Takashi Daiho, Stefania Danko, and Hiroshi Suzuki
Department of Biochemistry, Asahikawa Medical University, Asahikawa 078-8510, Japan

Running Title: Ca^{2+} release from $E1PCa_2$ of Ca^{2+}-ATPase

Correspondence address to: Kazuo Yamasaki, Dept. of Biochemistry, Asahikawa Medical University, Midorigaoka-Higashi, Asahikawa, 078-8510, Japan, Tel.: +81-166-68-2353; Fax: +81-166-68-2359; E-mail: kyamasak@asahikawa-med.ac.jp.

During Ca^{2+} transport by sarcoplasmic reticulum Ca^{2+}-ATPase, the conformation change of ADP-sensitive phosphoenzyme ($E1PCa_2$) to ADP-insensitive phosphoenzyme ($E2PCa_2$) is followed by rapid Ca^{2+} release into the lumen. Here we find that, in the absence of K^+, Ca^{2+} release occurs considerably faster than $E1PCa_2$ to $E2PCa_2$ conformation change. Therefore the lumenal Ca^{2+} release pathway is open to some extent in the K^+-free $E1PCa_2$ structure. The Ca^{2+} affinity of this $E1P$ is as high as that of the unphosphorylated ATPase ($E1$), indicating the Ca^{2+} binding sites are not disrupted. Thus bound K^+ stabilizes the $E1PCa_2$ structure with occluded Ca^{2+}, keeping the Ca^{2+} pathway to the lumen closed. We found previously (*J. Biol. Chem.* 283, 29144-29155 (2008)) that the K^+ bound in $E2P$ reduces the Ca^{2+} affinity essential for achieving the high physiological Ca^{2+} gradient and to fully open the lumenal Ca^{2+} gate for rapid Ca^{2+} release ($E2PCa_2 \rightarrow E2P + 2Ca^{2+}$). These findings show that bound K^+ is critical for stabilizing both $E1PCa_2$ and $E2P$ structures thereby contributing to the structural changes that efficiently couple phosphoenzyme processing and Ca^{2+} handling.

Sarcoplasmic reticulum (SR[1]) Ca^{2+}-ATPase (SERCA1a) catalyzes Ca^{2+} transport coupled with ATP hydrolysis against ~10,000-fold concentration gradient (1-9). The ATPase is first activated by the binding of two cytoplasmic Ca^{2+} ions at the transport sites with a submicromolar high affinity ($E2$ to $E1Ca_2$, step 1 in Fig. 1), then auto-phosphorylated at Asp^{351} by ATP to form a phosphoenzyme intermediate (EP) (step 2). This EP is "ADP-sensitive" ($E1$P) because it is rapidly dephosphorylated by ADP in the reverse reaction. Upon $E1$P formation, the bound Ca^{2+} ions are occluded in the transport sites ($E1PCa_2$). Subsequently, $E1PCa_2$ undergoes its isomeric transition to an ADP-insensitive form ($E2$P), *i.e.* loss of ADP-sensitivity, which results in a large reduction of Ca^{2+} affinity and opening of the lumenal release gate, *i.e.* Ca^{2+} deocclusion and release (steps 3-4). Ca^{2+} release in step 4 is very rapid, so that an $E2PCa_2$ intermediate state does not accumulate and in fact had never been found until we recently established its existence (10-13) and successfully trapped it for the first time (14). Finally, $E2$P is hydrolyzed back to the inactive $E2$ form (step 5).

In $E1PCa_2 \rightarrow E2P + 2Ca^{2+}$, the A domain rotates parallel to the membrane plane and the P domain inclines to the A domain, thereby associating with each other to produce a compactly organized and inclined headpiece (15-27). This tight structure is stabilized by critical interaction networks between the A and P domains at three regions (10-14) (see details in Fig. 9). The rotation and inclination of the domains result in motions and rearrangements of the transmembrane helices thereby disrupting the Ca^{2+} sites and opening the lumenal gate. In the P domain, there is a specific K^+ binding site (28); K^+ binding here is crucial for rapid hydrolysis of $E2$P (28-30). Recently we further found (13) that the K^+ in $E2$P is critical for reducing the lumenal Ca^{2+} affinity that is required to achieve the high physiological Ca^{2+} gradient and for rapid Ca^{2+} release ($E2PCa_2 \rightarrow E2P + 2Ca^{2+}$). Thus, bound K^+ contributes to stabilization of the compactly organized and inclined $E2$P structure with its disrupted Ca^{2+} sites and fully opened lumenal gate, probably by cross-linking the P domain with the A domain/M3-linker (13).

Despite these findings on the Ca^{2+} release process and $E2$P, a possible role for K^+ in $E1PCa_2$ has not been explored. The K^+ site is situated at the bottom of the P-domain near the cytoplasmic ends of the transmembrane helices. Therefore the lack of K^+ binding might have a serious effect on the stability of the helices and Ca^{2+}-handling in $E1PCa_2$. The $E2$-$E1Ca_2$ transition is markedly retarded and its equilibrium affected by the absence of K^+ (31-33).

In this study, we explore a possible role of K^+ in $E1PCa_2$ especially in regard to Ca^{2+} occlusion. Results reveal that K^+-free $E1PCa_2$ has an open Ca^{2+} pathway to the lumen. Thus the Ca^{2+} binding sites face the lumen and Ca^{2+} can be

released. The absence of K^+ does not reduce the high Ca^{2+} affinity (Ca^{2+} site coordination probably unchanged) and yet the cytoplasmic gate is closed and the lumenal one open. These changes probably do not involve large motions of the cytoplasmic domains and transmembrane helices. Therefore bound K^+ likely stabilizes the Ca^{2+} occluded structure of $E1PCa_2$ by simply keeping the lumenal Ca^{2+} pathway closed. The structural role of K^+ in $E1PCa_2$ is discussed in detail using crystal structures of Ca^{2+}-ATPase with bound K^+.

EXPERIMENTAL PROCEDURES

Preparation of SR Vesicles — SR vesicles were prepared from rabbit skeletal muscle as described (34). The phosphorylation site content in the vesicles determined according to Barrabin *et al.* (35) was 4.49 ± 0.22 nmol/mg vesicle protein (n = 5).

Determination of EP — SR vesicles were phosphorylated with [γ-^{32}P]ATP as described in the legends for Figs. 2-6. In the experiments performed in Fig. 2, aliquots of the reaction mixture were spotted on the HAWP membrane filter (Millipore) and washed continuously with a chasing solution for the periods indicated. At the end of chase, the reaction was terminated by washing with 0.1 M HCl. To determine the amount of $E2P$ in the phosphorylation mixture, the membrane was washed with an ADP solution for 1 s and then with 0.1 M HCl. The membrane was dried and the radioactivity measured by digital autoradiography. In Figs. 3 and 6, total EP was measured by quenching the phosphorylation reaction (in a test tube) with 5% (v/v) ice-cold trichloroacetic acid containing P_i, while for $E2P$ determination, the reaction was chased with ADP for 1 s and quenched by addition of the trichloroacetic acid. The precipitated proteins were separated by 5% SDS-PAGE at pH 6.0 according to Weber and Osborn (36). The radioactivity associated with the separated Ca^{2+}-ATPase was quantitated by digital autoradiography (37). Rapid kinetic measurements in Fig. 3 were performed with a handmade rapid mixing apparatus (38).

Determination of Bound Ca^{2+} — In the experiments performed in Figs. 2 and 6, SR vesicles were incubated with $^{45}CaCl_2$ as per the figure legends, and an aliquot of reaction mixture was spotted on the HAWP membrane filter (Millipore). Then the membrane was perfused with a chasing solution for indicated time periods using a rapid filtration apparatus RFS-4 (Bio-Logic, Claix, France). To estimate the non-specific $^{45}Ca^{2+}$ binding, the same experiments were done in the presence of 1 μM thapsigargin. Specific $^{45}Ca^{2+}$ binding was obtained after subtracting this non-specific binding.

Ca^{2+} Uptake into SR Vesicles in a Single Turnover of EP — In the experiments performed in Figs. 4 and 5, SR vesicles were incubated with $^{45}Ca^{2+}$, and a single turnover of EP was initiated by adding ATP and excess EGTA using the handmade rapid mixing apparatus. After chasing the reaction, the mixture was spotted on the membrane filter and washed for ~10 s by an EGTA solution, as described in the figure legends. The background level of $^{45}Ca^{2+}$ was determined without ATP, and subtracted. This background level was less than 3% of the maximum Ca^{2+} uptake level.

Miscellaneous — All the reactions were performed at 4 °C in 7 mM $MgCl_2$ and 50 mM MOPS/Tris (pH 7.3). Protein concentrations were determined by the method of Lowry *et al.* (39) with bovine serum albumin as a standard. Free Ca^{2+} concentrations were calculated by the Calcon program. Data were analyzed by nonlinear regression using the program Origin (Microcal Software, Inc., Northampton, MA). Three-dimensional models of the enzyme were produced by the program VMD (40).

RESULTS

Time Courses of EP Decay and Ca^{2+} Release — The Ca^{2+}-ATPase in SR vesicles was phosphorylated with MgATP in the presence of 0.1 M K^+, 10 μM Ca^{2+}, and Ca^{2+}-ionophore A23187 (Fig. 2*A*, *B*). The reaction reaches steady state within a few seconds and almost all of Ca^{2+}-ATPase is in the ADP-sensitive form of EP ($E1P$) because of the rate-limiting $E1P$ to $E2P$ transition followed by rapid $E2P$ hydrolysis in the presence of K^+ (29, 30).

When the reaction was chased with excess EGTA in 0.1 M K^+, the amount of EP decreases in a single-exponential time course, and the EP during the decay is almost all ADP-sensitive (Fig. 2*A*). The bound Ca^{2+} decreases concomitantly with $E1P$ decay, *i.e.* $E1PCa_2$ to $E2P$ transition. The result agrees with the established mechanism that the two Ca^{2+} ions are occluded in $E1PCa_2$ and Ca^{2+} release into the lumen occurs very rapidly after the rate-limiting $E1PCa_2$ to $E2PCa_2$ transition, $E1PCa_2 \rightarrow E2PCa_2 \rightarrow E2P + 2Ca^{2+}$ (11-14). Thus the EP

transition and Ca^{2+} release are tightly coupled in the presence of K^+.

Surprisingly, when $E1PCa_2$ formed as above in 0.1 M K^+ and A23187 was chased with excess EGTA in the absence of K^+, the Ca^{2+} release is considerably (~3-times) faster than the $E1P$ decay via its transition to $E2P$ (Fig. 2*B*). The result shows that in the absence of K^+, there is an $E1P$ species without bound Ca^{2+} and that the Ca^{2+} ions are released from $E1PCa_2$. We found essentially the same results in the presence of choline-Cl in place of LiCl without K^+ (data not shown).

$^{45}Ca^{2+}$ Uptake in Single Turnover of $E1PCa_2$ — We then examined whether this rapid Ca^{2+} release from $E1PCa_2$ in the absence of K^+ upon the EGTA chase occurs to the lumenal side or cytoplasmic side of the membrane. For this purpose, we performed a $^{45}Ca^{2+}$ uptake assay in a single turnover of $E1PCa_2$ in the absence of ionophore, *i.e.* with sealed SR vesicles. In Fig. 3 for the single turnover of $E1PCa_2$, the Ca^{2+}-ATPase in the vesicles in 10 μM Ca^{2+} was phosphorylated by a simultaneous addition of [γ-^{32}P]ATP and excess EGTA in either the presence or the absence of 0.1 M K^+. Approximately half of the ATPase is phosphorylated rapidly to form $E1PCa_2$ both in the presence and absence of K^+ and then EP decays slowly, in contrast to the full phosphorylation achieved without the removal of Ca^{2+}. In sealed vesicles (without A23187), EP decays at the same rate in the presence or absence of K^+. In the presence of K^+, nearly all EP is $E1P$ (ADP-sensitive), while in the absence of K^+, $E2P$ increases slowly to approximately 20% at ~2 s of the maximum amount of EP formed immediately after the ATP addition.

Then in Fig. 4 *closed circles*, the $^{45}Ca^{2+}$ uptake assay during a single turnover of $E1PCa_2$ was performed by membrane filtration with an EGTA chase, *i.e.* with extensive EGTA washing of the filter for ~10 s under otherwise the same conditions as in the single turnover of $E1PCa_2$ in Fig. 3. During the ~10 s of EGTA washing, nearly all EP is dephosphorylated (Fig. 3) as we intended, therefore all the bound $^{45}Ca^{2+}$ in EP has been released even at the first time point (0.1 s after the start when nearly all EP is $E1PCa_2$) either to the cytoplasmic side or lumenal side. If released to the cytoplasmic side, the $^{45}Ca^{2+}$ will be lost from the filter by the EGTA-wash and levels will be reduced significantly from the ideal stoichiometry of two Ca^{2+} ions transported in a single turnover of $E1PCa_2$. However the results (*closed circles*) clearly show a maximum uptake of ~1.7 Ca^{2+} per EP in 0.1 M K^+ and an even higher uptake of 1.8~1.9 without K^+, very close to the ideal stoichiometry. Therefore during a single turnover, the bound $^{45}Ca^{2+}$ ions in $E1PCa_2$ formed in the absence of K^+ are not released to the cytoplasmic side but to the lumen. It is concluded that in $E1PCa_2$ without K^+, the cytoplasmic gate is closed but a Ca^{2+} pathway to the lumen exists. Thus the Ca^{2+} binding sites face the lumen.

ADP-chase during Single Turnover of $^{45}Ca^{2+}$ Uptake — In Fig. 4 *open circles*, we assessed at each time point during the single turnover of $E1PCa_2$ the amount of $^{45}Ca^{2+}$ remaining on the filter with the vesicles. For this purpose, we chased the reaction with ADP and excess EGTA at each time point, *i.e.* dephosphorylating to $E1Ca_2$ very rapidly in the reverse reaction and removing $^{45}Ca^{2+}$ released to the cytoplasmic side. Both in the presence and absence of K^+, at 0.1 s (first time point) immediately after the ATP/EGTA addition, nearly maximum EP is already formed (all $E1PCa_2$, Fig. 3) and all the bound $^{45}Ca^{2+}$ is removed by the ADP-chase. Then in the presence of 0.1 M K^+ (*A*), the ADP-insensitive fraction and the amount of $^{45}Ca^{2+}$ released into the lumen increased exponentially due to the forward $E1PCa_2$ decay via its transition to $E2P$ with Ca^{2+} release as expected from the established transport mechanism. In fact, the time course agreed with that of EP decay via the rate-limiting $E1PCa_2$ to $E2P$ transition (Fig. 3, *closed triangles*).

On the other hand, in the absence of K^+ (*B*), $^{45}Ca^{2+}$ and the ADP-insensitive fraction increase very rapidly (within the initial ~0.5 s) and suddenly slow, showing a clear biphasic time course. The second slow phase occurs at nearly the same rate as the EP decay via the $E1P$ to $E2P$ transition (Fig. 3, *open triangles*) and the single exponential $^{45}Ca^{2+}$ uptake in the presence of K^+ (*A*), *i.e.* the normal transport process $E1PCa_2 \rightarrow E2PCa_2 \rightarrow E2P + 2Ca^{2+}$. The initial rapid phase occurs at a significantly faster rate and to a higher extent than in $E2P$ formation (Fig. 3), and therefore cannot be accounted for simply by formation of $E2P$. Actually, the initial phase is even faster than the Ca^{2+} release from K^+-free $E1PCa_2$ revealed upon excess EGTA addition (without ADP) in A23187 in Fig. 2. The results suggest that, in K^+-free $E1PCa_2$, different types of Ca^{2+} sites are produced in the initial rapid phase; the Ca^{2+} ions are not released

to the cytoplasmic side even upon ADP-induced reverse dephosphorylation.

Behavior of $^{45}Ca^{2+}$ at Site I in E1PCa$_2$ — We examined if the above observed biphasic kinetics revealed by the ADP-chase is related to the heterogeneity of the Ca^{2+} sites I and II in *E*1Ca$_2$. In *E*1Ca$_2$, Ca^{2+} bound at site II is rapidly exchanged with the cytoplasmic Ca^{2+}, and the Ca^{2+} bound at the deeper site I can be released to the cytoplasm only when site II is vacant (15, 41-44). Therefore, we first labeled site I with $^{45}Ca^{2+}$ by exchanging the site II-bound $^{45}Ca^{2+}$ with non-radioactive Ca^{2+} (supplemental Fig. S1). In Fig. 5*B*, we clearly observe a biphasic $^{45}Ca^{2+}$ increase in the ADP-insensitive fraction in the absence of K^+ as in Fig. 4*B*. The only difference is that, as expected, the total amount of $^{45}Ca^{2+}$ uptake (0.8-1.0 Ca^{2+} per *E*P) is half of that in Fig. 4 in which both sites I and II are labeled by $^{45}Ca^{2+}$. The results show that the heterogeneity of the two Ca^{2+} sites I and II in *E*1Ca$_2$ is not related to the biphasic $^{45}Ca^{2+}$ increase revealed by the ADP-chase in Fig. 4*B*. Furthermore, we observed a non-sequential release of two Ca^{2+} ions from *E*1PCa$_2$ to the lumenal side upon removal of free Ca^{2+} in the presence of A23187 without ADP, which therefore is not related to the biphasic $^{45}Ca^{2+}$ increase in Fig. 4*B* (supplemental Figure S2 with additional references 58, 59).

These results show that there are two different types of *E*1PCa$_2$, *i.e.* the normal Ca^{2+}-occluded *E*1PCa$_2$ and another *E*1PCa$_2$ species that possesses lumen-facing Ca^{2+} binding sites (opened lumenal pathway) and a closed cytoplasmic gate. The results further indicate that in the absence of K^+, the *E*1PCa$_2$ species with the lumen-facing Ca^{2+} binding sites is rapidly produced from normal *E*1PCa$_2$, and this process is revealed by the ADP-chase as the initial rapid phase in Fig. 4*B* (see more in "DISCUSSION" and a schematic model in Fig. 7).

Affinity of E1P for Lumenal Ca^{2+} in the Absence of K^+ — In Fig. 6, we assess the Ca^{2+} affinity of the transport sites exposed to the lumen in K^+-free *E*1PCa$_2$ by determining the Ca^{2+} binding to *E*1P in steady state in the presence of A23187. In Fig. 6*A*, the total amount of *E*P increased with increasing Ca^{2+} concentration and reached its maximum level at ~0.5 μM Ca^{2+} due to high affinity Ca^{2+} binding at the transport sites (*E*2 to *E*1Ca$_2$ transition). The total amount of *E*P at saturating Ca^{2+} was half of the maximum Ca^{2+} binding in *E*1Ca$_2$ (*B*), therefore all Ca^{2+}-ATPases are phosphorylated at saturating Ca^{2+}. As replotted in Fig. 6*C*, approximately 60% of the maximum total amount of *E*P was *E*1P in steady state at saturating Ca^{2+} under these conditions.

In Fig. 6*B*, the amount of bound Ca^{2+} in steady state in the presence of A23187 was determined without washing the filter so as not to alter the equilibrium. As replotted in Fig. 6*C* with %values relative to the maximum Ca^{2+} binding in *E*1Ca$_2$, the bound Ca^{2+} under the phosphorylating condition without K^+ increases concomitantly with an increase in *E*1P, and their relative values are nearly the same. Note that if the affinity of the lumen-facing Ca^{2+} sites of *E*1P without K^+ is significantly lower than that of the high Ca^{2+} affinity in *E*1 for the phosphorylation, the Ca^{2+} binding curve would be shifted significantly to higher Ca^{2+} concentrations, and the relative value of the bound Ca^{2+} would become significantly smaller than that of *E*1P in the ~μM range. However, this is obviously not the case. We conclude that the affinity of the lumen-facing Ca^{2+} sites of K^+-free *E*1P is as high as the cytoplasmic Ca^{2+} affinity in *E*1.

DISCUSSION

Ca^{2+}-release from E1PCa$_2$ in the Absence of K^+ — Our studies show that in the absence of K^+, Ca^{2+} is released from *E*1PCa$_2$ to the lumenal side. This Ca^{2+} release obviously precedes the conversion of the ADP-sensitive *E*P (*E*1P) to ADP-insensitive one (*E*2P), thus there is a K^+-free *E*1P species without bound Ca^{2+} (Fig. 2*B*). Evidently a Ca^{2+} pathway from the transport sites to the lumen is open at least to some extent in this species. K^+, probably bound to its specific site in the ATPase (28), therefore plays a critical role in *E*1PCa$_2$ to stabilize the transport sites in an occluded state. Notable also is our finding that the Ca^{2+} affinity of the sites facing the lumen in K^+-free *E*1PCa$_2$ is as high as the cytoplasmic Ca^{2+} affinity in the unphosphorylated *E*1 state (Fig. 6). Thus the Ca^{2+} binding sites are not disrupted in this K^+-free *E*1PCa$_2$ structure, suggesting that the opening of the lumenal Ca^{2+} pathway does not involve large structural changes such as occur during the *E*P conformation change. The observation also means that such a Ca^{2+}-ATPase species cannot be involved in producing a Ca^{2+} gradient across the membrane and therefore is unlikely to contribute significantly to active

Ca^{2+} transport. This is because, without a reduction in Ca^{2+} affinity, lumenal Ca^{2+} would rebind at low concentrations and inhibit the pump.

Our kinetic analysis of the lumenal Ca^{2+}-induced reverse conversion $E2P + 2Ca^{2+} \leftrightarrow E2PCa_2 \leftrightarrow E1PCa_2$ in wild type Ca^{2+}-ATPase (13) has revealed that the K^+ in $E2P$ is critical for lowering the lumenal Ca^{2+} affinity and for fully opening the lumenal gate, thereby accomplishing the high physiological Ca^{2+} gradient and rapid Ca^{2+} release $E2PCa_2 \rightarrow E2P + 2Ca^{2+}$. K^+ stabilizes the $E2P$ structure with disrupted Ca^{2+} sites and a fully open lumenal gate. In the absence of K^+, the lumenal Ca^{2+} affinity of $E2P$ is ~2000 times lower than in $E1P$ ($K_{0.5}$ values 0.4 mM (13) and 0.15 μM (Fig. 6), respectively). Therefore, the large structural change associated with the EP conformation change is obviously required, even in the absence of K^+, for disrupting the Ca^{2+} sites. K^+ binding in $E2PCa_2/E2P$ further reduces the Ca^{2+} affinity to a level ($K_{0.5}$ value 1.5 mM (13)) appropriate for producing the high physiological Ca^{2+} gradient across the membrane.

Thus, bound K^+ stabilizes both the Ca^{2+} occluded structure of $E1PCa_2$ and the Ca^{2+}-released structure of $E2P$. Thereby K^+ critically contributes to the successive structural changes and ensures strict and efficient coupling for EP processing and Ca^{2+} handling in $E1PCa_2 \rightarrow E2PCa_2 \rightarrow E2P + 2Ca^{2+}$, key events for Ca^{2+} transport. Also notable is the fact that the K^+ bound in the P domain is crucial for producing a catalytic-site structure in $E2P$ appropriate for its accelerated hydrolysis (28-30).

Biphasic Ca^{2+}-release in ADP-chase of Single turnover of $E1PCa_2$ without K^+ — In Fig. 7, we provide a schematic model to show the roles of K^+ in the Ca^{2+} transport and to account for the biphasic Ca^{2+} release from K^+-free $E1PCa_2$ following an ADP-chase during a single turnover (Fig. 4*B*, *open circles*). The fast initial phase may be accounted for by the rapid formation of s$E1PCa_2$, with lumen-facing, high affinity Ca^{2+} binding sites, in rapid equilibrium with normal $E1PCa_2$. The bound $^{45}Ca^{2+}$ ions cannot be released to the cytoplasmic side even upon ADP-induced reverse dephosphorylation (s$E1Ca_2$) but only to the lumenal side (*yellow arrow*). Since s$E1P$ has high affinity, Ca^{2+} rebinding occurs at low lumenal concentrations[2] and inhibits flux through this pathway. The slow second phase (Fig. 4*B*) most probably reflects the $E1PCa_2$ to $E2P$ transition as in the single exponential Ca^{2+} uptake in 0.1 M K^+ (Fig. 4*A*, *blue arrows* in Fig. 7). The formation of s$E1PCa_2$ in rapid equilibrium with occluded $E1PCa_2$ necessarily lowers the steady state level of the latter species and hence Ca^{2+} transport through the normal route. Thus, although progression to s$E1PCa_2$ is relatively fast this pathway cannot contribute to gradient formation and ultimately slows normal transport. It is concluded that K^+ ensures the normal structural process for Ca^{2+} transport (*blue arrows*) by stabilizing the Ca^{2+} occluded structure of $E1PCa_2$ and disallowing opening of a lumenal Ca^{2+} pathway (this study), and by stabilizing the $E2P$ structure with disrupted Ca^{2+} sites (greatly reduced affinity) and a fully opened lumenal gate (13).

Structural Role of Bound K^+ in $E1PCa_2$ — The crystal structures provide a likely structural role of bound K^+ in $E1PCa_2$. In structures analogous to K^+-bound $E1PCa_2$ ($E1PCa_2$·AMPPN (22) and $E1Ca_2$·AlF_4^-·ADP as well as $E1Ca_2$·AMPPCP (17)), K^+ is specifically bound at the bottom part of the P domain and coordinated by the backbone carbonyl oxygens of Leu^{711}, Lys^{712}, and Ala^{714} on Pα6 (6th P-domain α-helix) (near the catalytic Mg^{2+} site Asp^{703}/Asp^{707} on Pα5 of this region) and by the Glu^{732} side chain oxygen on Pα7 (Fig. 8). The importance of Glu^{732} in the K^+-induced acceleration of $E2P$ hydrolysis was shown through mutations (28).

The K^+ ion and these ligands are distant from and not in direct contact with the transport sites from which Ca^{2+} release occurs. On the other hand, adjacent to the K^+ binding site on Pα6/Pα7 is Pα1, which is directly linked with the cytoplasmic end of M4 within the P domain. Pα6, Pα7, and Pα1 constitute the bottom part of one half of the P domain and move together as a body during the transport cycle (7, 18). Furthermore, Pα1 forms a hydrogen-bonding network with L6-7 (a cytoplasmic short loop linking M6 and M7) and top parts of M3/M5. This interaction network is critical for proper arrangement of the transmembrane helices (48-50). In fact, disruption of this network by mutations causes a marked retardation of the $E2$-$E1$ transition (48, 49).

Since the bound K^+ is deeply embedded and ligated within this part of the P-domain (Fig. 8*a*), its absence would allow more flexibility of the structural components, such as segmental fluctuations or wobbling, which in turn would impinge on the cytoplasmic regions of the

transmembrane helices and probably destabilize the interaction network Pα1/L6-7/M3/M5. The absence of K^+ in fact markedly retards the *E*2 to *E*1 transition (31, 32) and, as noted above, disruption of the Pα1/M3/M5/L6-7 interaction network markedly retards the *E*1-*E*2 transition and also the *E*1P to *E*2P conformation change (48-50). Opening of the lumenal pathway and Ca^{2+} release from *E*1PCa_2 may be caused by such structural perturbations in the absence of bound K^+.

As shown in the view from the lumen of the helices M4/M5/M6/M8 ligating Ca^{2+} in Fig. 8*c*, the space surrounded by these helices seems to be the only possible Ca^{2+} exit pathway. M3 is in close contact at the lumenal end with the lumenal part of M4 (M4L) and they are connected by a short lumenal loop (L3-4). During the *E*P conformation change and subsequent Ca^{2+} release (*E*1PCa_2 → *E*2P + $2Ca^{2+}$), M3 and M4L incline together and move outward, thereby opening the putative Ca^{2+} release pathway (lumenal gate) (19). The M3/M4L motion is produced by the large rotation and inclination of the A and P domains and by the consequent significant motions and rearrangements of the helices M1~M6, in which M1/M2 as a rigid body pushes M4L to open the Ca^{2+} release gate (19) (see Fig. 9). The large motions concomitantly disrupt the Ca^{2+} binding sites and reduce the Ca^{2+} affinity (19). In K^+-free *E*1PCa_2 (ADP-sensitive) these domain motions have not yet taken place and the Ca^{2+} sites are not disrupted and maintain a high affinity. Here these motions are likely much less prominent and opening of the release pathway is simply the result of fluctuations and wobbling of the relevant helices, in particular M3/M4L.

The unique Ca^{2+} coordination and particular make up of the M3 and M4 helices lend themselves to creating a release pathway while maintaining a high affinity. The Ca^{2+} sites with properly positioned ligands are located at an unwound portion of the M4 helix creating intrinsic flexibility (Fig. 8). On the other hand, M3 is a continuous helix from the cytoplasmic to the lumenal end, and is located at the periphery of the transmembrane domain and is not closely associated with other helices including M1/M2 (except for M4L at the lumenal end). Thus in the crystal structures analogous to *E*1PCa_2, M3 seems not to have much steric restriction against possible outward movement, a shift which would open the Ca^{2+} pathway. Therefore, if the cytoplasmic region of M3 is not fixed as occurs in the absence of bound K^+, its lumenal part and the associated M4L may become more mobile. Wobbling here could allow the Ca^{2+} pathway to fluctuate between a closed and open state. The Ca^{2+} sites are not necessarily disrupted because of the flexibility of the unwound structure of M4 and because the large motions of the A-P domains do not occur (these are the motions which disrupt the Ca^{2+} sites by inclining the cytoplasmic region of M4/M5). Also, M3 is not involved directly in the Ca^{2+} ligation.

Interestingly at the lumenal end of M4L (Fig. 8*c*), there are bulky and hydrophobic residues (Tyr^{294}/Tyr^{295}/Lys^{297}) which may form hydrogen-bonds, *e.g.* Tyr^{294}/Tyr^{295} with Glu^{785} on L4-5. Lys^{297} seems to seal the Ca^{2+}-channel (51). Tyr^{295} is important for Ca^{2+} transport activity and stabilizing *E*2 relative to *E*1 (52). These residues may possibly function as the lumenal plug, and M3/M4L-wobbling may destabilize their interactions helping to open the Ca^{2+} pathway in K^+-free *E*1PCa_2.

Importantly, in the crystal structures of analogues of *E*1PCa_2 the cytoplasmic Ca^{2+} gate is closed by the Ca^{2+} ligand Glu^{309} because Leu^{65} on M1 locks the Glu^{309} side chain configuration by van der Waals contact (8, 9, 18, 53). Our observation shows that this cytoplasmic gate is closed in *E*1PCa_2 even without bound K^+ and therefore the Glu^{309}-gating with Leu^{65} has not been affected.

Movement of K^+-binding Site during E1PCa_2 → E2P + $2Ca^{2+}$ — K^+-bound crystal structures *E*1PCa_2·AMPPN and *E*2·AlF_4^- may be used as a model for the overall change in *E*1PCa_2 → *E*2P + $2Ca^{2+}$ (Fig 9). Hence, the P domain inclines to the A domain that also rotates and inclines (*curved arrows*), thus producing the A-P domain association in the most compactly organized and inclined headpiece structure, the Ca^{2+}-released *E*2P. With this change, the cytoplasmic region of M4/M5 in the P domain inclines and disrupts the Ca^{2+} sites (19). M2 inclines with the A-domain motion and consequently M1, which forms a rigid V-shaped body with M2, pushes against the lumenal part of M4 and opens the lumenal gate (19).

In these structural changes, the K^+ site with bound K^+ on the P domain moves down to the Gln^{244} region on the A/M3-linker (*blue arrow*) and brings in the Gln^{244} side chain (or neighboring residues) as an additional coordination ligand. Thus bound K^+ likely cross-links the bottom part of the P domain and

the A/M3-linker. This cross-link must contribute to the stabilization of the compactly organized and inclined *E*2P structure with disrupted Ca^{2+} sites and fully opened lumenal gate (13).

The A/M1'-linker of correct length has a critical function in inclining and compacting the *E*2P structure (14, 27). The structure is stabilized by three critical interaction networks; at the Tyr^{122}-HC (hydrophobic interaction cluster involving the A and P domains and M2), at the Val^{200}-loop (ionic and hydrogen bonding interactions with the P domain residues), and at $TGES^{184}$ (hydrogen bonding interactions) (10-14). The $TGES^{184}$ loop of the rotated A domain protrudes into the catalytic site and blocks attack of ADP on the Asp^{351}-phosphate (causing the loss of ADP-sensitivity). The Tyr^{122}-HC is produced upon A-P domain inclination induced by tension on the A/M1'-linker (14, 27) and is critical for reducing the Ca^{2+} affinity and opening the lumenal gate, *i.e.* to deocclude/release Ca^{2+}, $E2PCa_2 \rightarrow E2P$ (11-13). All the interaction networks are essential for these changes and are also necessary for the formation of the catalytic site with hydrolytic activity (10-13). Importantly, the Val^{200}-loop and Tyr^{122}-HC are situated at the top and bottom of the A-P domain interface respectively, and bound K^+ is lower down and close to the membrane domain. Thus these interaction networks including the K^+ site are situated at positions most appropriate for stabilizing the compactly organized and inclined (thus strained) structure of *E*2P.

Ca^{2+} Release into Cytoplasm and Uncoupling — It was previously observed with SR Ca^{2+}-ATPase (54-57) that Ca^{2+} in $E1PCa_2$ can be released to cytoplasm upon direct hydrolysis to $E1Ca_2$ (not via its transition to *E*2P) under specific conditions such as with a raised lumenal Ca^{2+} level. This causes ATP hydrolysis without Ca^{2+} transport resulting in uncoupling. de Meis and co-workers further suggested (54-56) that such uncoupled ATP hydrolysis functions as a heat-producing entity. This finding obviously differs from ours in that in K^+-free $E1PCa_2$ the Ca^{2+} release pathway into the lumen is open and the phosphoenzyme not directly hydrolyzed.

In summary, we have found that $E1PCa_2$ without bound K^+ has a perturbed structure with at least a partially open lumenal Ca^{2+} release pathway and yet still with the Ca^{2+} sites maintaining a high affinity. Thus in the natural $E1PCa_2$ structure bound K^+ stabilizes the Ca^{2+} in an occluded form by not allowing the pathway to open. Bound K^+ also stabilizes *E*2P following disruption of the Ca^{2+} sites and full opening of the lumenal gate (13). Thus bound K^+ has a crucial role in *E*P processing and Ca^{2+} occlusion and release to the lumen in the sequence $E1PCa_2 \rightarrow E2PCa_2 \rightarrow E2P + 2Ca^{2+}$.

Acknowledgments — We are grateful to Dr. Chikashi Toyoshima, University of Tokyo, for helpful discussions. We thank Dr. David B. McIntosh for reviewing and improving our manuscript.

REFERENCES

1. Hasselbach, W., and Makinose, M. (1961) *Biochem. Z.* **333,** 518-528
2. Ebashi, S., and Lipmann, F. (1962) *J. Cell Biol.* **14,** 389-400
3. Inesi, G., Sumbilla, C., and Kirtley, M. E. (1990) *Physiol. Rev.* **70,** 749-776
4. Møller, J. V., Juul, B., and le Maire, M. (1996) *Biochim. Biophys. Acta* **1286,** 1-51
5. MacLennan, D. H., Rice, W. J., and Green, N. M. (1997) *J. Biol. Chem.* **272,** 28815-28818
6. McIntosh, D. B. (1998) *Adv. Mol. Cell Biol.* **23A,** 33-99
7. Toyoshima, C., and Inesi, G. (2004) *Annu. Rev. Biochem.* **73,** 269-292
8. Toyoshima, C. (2008) *Arch. Biochem. Biophys.* **476,** 3-11
9. Toyoshima, C. (2009) *Biochim. Biophys. Acta* **1793,** 941-946
10. Kato, S., Kamidochi, M., Daiho, T., Yamasaki, K., Wang, G., and Suzuki, H. (2003) *J. Biol. Chem.* **278,** 9624-9629
11. Yamasaki, K., Daiho, T., Danko, S., and Suzuki, H. (2004) *J. Biol. Chem.* **279,** 2202-2210
12. Wang, G., Yamasaki, K., Daiho, T., and Suzuki, H. (2005) *J. Biol. Chem.* **280,** 26508-26516
13. Yamasaki, K., Wang, G., Daiho, T., Danko, S., and Suzuki, H. (2008) *J. Biol. Chem.* **283,** 29144-29155
14. Daiho, T., Yamasaki, K., Danko, S., and Suzuki, H. (2007) *J. Biol. Chem.* **282,** 34429-34447
15. Toyoshima, C., Nakasako, M., Nomura, H., and Ogawa, H. (2000) *Nature* **405,** 647-655
16. Toyoshima, C., and Nomura, H. (2002) *Nature* **418,** 605-611

17. Sørensen, T. L-M., Møller, J. V., and Nissen, P. (2004) *Science* **304,** 1672-1675
18. Toyoshima, C., and Mizutani, T. (2004) *Nature* **430,** 529-535
19. Toyoshima, C., Nomura, H., and Tsuda, T. (2004) *Nature* **432,** 361-368
20. Olesen, C., Sørensen, T. L.-M., Nielsen, R. C., Møller, J. V., and Nissen, P. (2004) *Science* **306,** 2251-2255
21. Toyoshima, C., Norimatsu, Y., Iwasawa, S., Tsuda, T., and Ogawa, H. (2007) *Proc. Natl. Acad. Sci. U. S. A.* **104,** 19831-19836
22. Olesen, C., Picard, M., Winther, A.-M. L., Gyrup, C., Morth, J. P., Oxvig, C., Møller, J. V., and Nissen, P. (2007) *Nature* **450,** 1036-1042.
23. Danko, S., Daiho, T., Yamasaki, K., Kamidochi, M., Suzuki, H., and Toyoshima, C. (2001) *FEBS Lett.* **489,** 277-282
24. Danko, S., Yamasaki, K., Daiho, T., Suzuki, H., and Toyoshima, C. (2001) *FEBS Lett.* **505,** 129-135
25. Danko, S., Yamasaki, K., Daiho, T., and Suzuki, H. (2004) *J. Biol. Chem.* **279,** 14991-14998
26. Danko, S., Daiho, T., Yamasaki, K., Liu, X., and Suzuki, H. (2009) *J. Biol. Chem.* **284,** 22722-22735
27. Daiho, T., Danko, S., Yamasaki, K., and Suzuki, H. (2010) *J. Biol. Chem.* **285,** 24538-24547
28. Sørensen, T. L-M., Clausen, J. D., Jensen, A.-M. L., Vilsen, V., Møller, J. V., Andersen, J. P., and Nissen, P. (2004) *J. Biol. Chem.* **279,** 46355-46358
29. Shigekawa, M., and Pearl, L. J. (1976) *J. Biol. Chem.* **251,** 6947-6952
30. Shigekawa, M., and Dougherty, J. P. (1978) *J. Biol. Chem.* **253,** 1451-1457
31. Medda, P., Fassold, E., and Hasselbach, W. (1987) *Eur. J. Biochem.* **165,** 251-259
32. Lee, A. G., Baker, K., Khan, Y. M., and East J. M. (1995) *Biochem. J.* **305,** 225-231
33. Champeil, P., Henao, F., and de Foresta, B. (1997) *Biochemistry* **36,** 12383-12393
34. Nakamura, S., Suzuki, H., and Kanazawa, T. (1994) *J. Biol. Chem.* **269,** 16015-16019
35. Barrabin, H., Scofano, H. M., and Inesi, G. (1984) *Biochemistry* **23,** 1542-1548
36. Weber, K., and Osborn, M. (1969) *J. Biol. Chem.* **244,** 4406-4412
37. Daiho, T., Suzuki, H., Yamasaki, K., Saino, T., and Kanazawa, T. (1999) *FEBS Lett.* **444,** 54-58
38. Kanazawa, T., Saito, M., and Tonomura, Y. (1970) *J. Biochem*. (*Tokyo*) **67,** 693-711
39. Lowry, O. H., Rosebrough, N. J., Farr, A. L., and Randall, R. J. (1951) *J. Biol. Chem.* **193,** 265-275
40. Humphrey, W., Dalke, A., and Schulten, K. (1996) *J. Mol. Graphics* **14,** 33-38
41. Nakamura, J. (1989) *J. Biol. Chem.* **264,** 17029-17031
42. Inesi, G. (1987) *J. Biol. Chem.* **262,** 16338-16342
43. Petithory, J. R., and Jencks, W. P. (1988) *Biochemistry* **27,** 8626-8635
44. Orlowski, S., and Champeil, P. (1991) *Biochemistry* **30,** 352-361
45. Malan, N. T., Sabbadini, R., Scales, D., and Inesi, G. (1975) *FEBS Lett.* **60,** 122-125
46. Duggan, P.F., and Martonosi, A. (1970) *J. Gen. Physiol.* **56,** 147-167
47. Fleischer, S., and Inui, M. (1989) *Annu. Rev. Biophys. Biophys. Chem.* **18,** 333-364
48. Clausen, J. D., and Andersen, J. P. (2004) *J. Biol. Chem.* **279,** 54426-54437
49. Lenoir, G., Picard, M., Møller, J. V., le Maire, M., Champeil, P., and Falson, P. (2004) *J. Biol. Chem.* **279,** 32125-32133
50. Zhang, Z., Lewis, D., Sumbilla, C., Inesi, G., and Toyoshima, C. (2001) *J. Biol. Chem.* **276,** 15232-15239
51. Chen, L., Sumbilla, C., Lewis, D., Zhong, L., Strock, C., Kirtley, M. E., and Inesi, G. (1996) *J. Biol. Chem.* **271,** 10745-10752
52. Lee, A. G. (2002) *Biochim. Biophys. Acta* **1565,** 246-266
53. Einholm, A. P., Vilsen, B., and Andersen, J. P. (2004) *J. Biol. Chem.* **279,** 15888-15896
54. de Meis, L. (2001) *J. Biol. Chem.* **276,** 25078-25087
55. Reis, M., Farage, M., Souza, A. C. L., and de Meis, L. (2001) *J. Biol. Chem.* **276,** 42793-42800
56. Barata, H., and de Meis, L. (2002) *J. Biol. Chem.* **277,** 16868-16872
57. Yu, X., and Inesi, G. (1995) *J. Biol. Chem.* **270,** 4361-4367
58. Hanel, A. M., and Jencks, W. P. (1991) *Biochemistry* **30,** 11320-11330
59. Orlowski, S., and Champeil, P. (1991) *Biochemistry* **30,** 11331-11342

FOOTNOTES

*This work was supported by a Grant-in-Aid for Scientific Research (C) (to K.Y.) and (B) (to H.S.) from the Ministry of Education, Culture, Sports, Science and Technology of Japan.

[1]The abbreviations used are: SR, sarcoplasmic reticulum; *E*P, phosphoenzyme; *E*1P, ADP-sensitive phosphoenzyme; *E*2P, ADP-insensitive phosphoenzyme; MOPS, 3-(*N*-morpholino) propanesulfonic acid.

[2]Note that the intravesicular volume of SR vesicles has been estimated to be in the range of 2-10 μl/mg protein (45, 46) and therefore the release of Ca^{2+} bound in *E*P (~8 nmol/mg protein) into the lumen in a single turnover might increase the lumenal Ca^{2+} to ~0.8-4 mM. Although a fair amount of lumenal free Ca^{2+} may be removed by low affinity Ca^{2+} buffers such as calsequestrin (47), even a small rise in the lumenal Ca^{2+} level might result in re-binding of lumenal Ca^{2+} to s*E*1P because of its high affinity revealed in Fig. 6 (*yellow arrow* in Fig. 7).

FIGURE LEGENDS

FIGURE 1. Reaction scheme of Ca^{2+}-ATPase

FIGURE 2. Time courses of *E*P decay and Ca^{2+} release in the presence or absence of 0.1 M K^+. *A*, The Ca^{2+}-ATPase in SR vesicles (20 μg protein/ml) was phosphorylated for 10 s with 100 μM [γ-^{32}P]ATP in 10 μM non-radioactive $CaCl_2$ (*closed circles* and, in *inset*, *triangles*), or with 100 μM non-radioactive ATP in 10 μM $^{45}CaCl_2$ (*open circles*), 0.1 M KCl, 3 μM A23187. Then 50 μl of the reaction mixture was spotted on the membrane and washed for the time periods on the abscissa with a chasing solution containing 1mM EGTA, 0.1 M KCl, 3 μM A23187. The amount of bound $^{45}Ca^{2+}$ (*open circles*) and the total amount of *E*P (*open triangles* in *inset*) were determined. The amounts of *E*2P (*closed triangles* in *inset*) were determined by a subsequent washing by a solution containing 1 mM ADP, 1 mM EGTA, and 0.1 M KCl. The amount of *E*1P (*closed circles*) was calculated by subtracting the amount of *E*2P from total amount of *E*P. *B*, the Ca^{2+}-ATPase in SR vesicles was phosphorylated in the presence of 0.1 M KCl as in *A*, and spotted on the filter. Then, the filter was washed with the EGTA solution (and subsequently with the ADP solution for the *E*2P determination) containing 0.1 M LiCl instead of KCl, otherwise as in *A*. *Solid lines* in the *main panel A* and *B* show the least squares fit to a single-exponential. The rates (s^{-1}) for the *E*1P decay and the Ca^{2+} release were 0.66 and 0.58 (*A*), and 0.21 and 0.81 (*B*), respectively.

FIGURE 3. *E*P formation and decay in a single turnover. All the solutions contained 0.1 M KCl (*closed symbols*) or LiCl (*open symbols*). SR vesicles (20 μg/ml) were incubated in 10 μM $CaCl_2$, and *E*P formation was initiated by mixing with an equal volume of a solution containing 20 μM [γ-^{32}P]ATP and 10 mM EGTA (*triangles* and *squares*) or 10 μM $CaCl_2$ (*circles*). The total amount of *E*P was determined with the addition of trichloroacetic acid (*circles* and *triangles*). To determine the amount of *E*2P (*squares*), the phosphorylated sample was mixed with an equal volume of a solution containing 2 mM ADP and 5 mM EGTA, and then the reaction was terminated by trichloroacetic acid at 1 s after the ADP addition.

FIGURE 4. $^{45}Ca^{2+}$ uptake in a single turnover of *E*P with and without K^+. All the solutions contained 0.1 M KCl (*A*) or LiCl (*B*). In the absence of Ca^{2+} ionophore, SR vesicles (20 μg/ml) were first incubated with 10 μM $^{45}CaCl_2$ for ~10 min, then Ca^{2+} uptake in a single turnover of *E*P was initiated by mixing with an equal volume of a solution containing 20 μM ATP and 2 mM EGTA, as in Fig. 3. After the indicated periods, the reaction was chased with an equal volume of a solution containing 2 mM EGTA without (*closed circles*) or with (*open circles*) 2 mM ADP. The mixture was immediately spotted on the membrane and washed for ~10 s by 1 ml of a 2 mM EGTA solution. The amount of $^{45}Ca^{2+}$ on the membrane, *i.e.* transported into the vesicles and/or remained bound to the ATPase and not released to cytoplasmic side, was normalized to the maximum total amount of *E*P formed immediately after the addition ATP and EGTA (Fig. 3). In *A*, the time course obtained with the ADP-chase was best described by a single-exponential Ca^{2+} uptake (*solid line*) with a rate constant of

0.49 s^{-1} and maximum Ca^{2+}/*E*P value of 1.26. In *B*, it was best described by a double-exponential (*broken line*) with a rate constant and maximum Ca^{2+}/*E*P value of 5.1 s^{-1} and 0.66 for the fast phase and 0.24 s^{-1} and 0.98 for the slow phase (but it was not described by a single-exponential increase shown by *solid line* with the rate constant 1.54 s^{-1} and the maximum value 1.31). Note also that, without the ADP addition, almost all the bound Ca^{2+} ions are transported into the vesicles during the ~10 s EGTA wash because the single turnover of *E*P is nearly completed in this period (see Fig. 3).

FIGURE 5. Uptake of Site I-bound $^{45}Ca^{2+}$ in a single turnover of *E*P with and without K^+. SR vesicles were incubated with 10 μM $^{45}Ca^{2+}$ as in Fig. 4, and diluted by an equal volume of a solution containing 2 mM non-radioactive $CaCl_2$, and 0.1 M KCl (*A*) or LiCl (*B*), and further incubated for 10 s. By this incubation, site I of the two Ca^{2+} sites (I, II) is labeled with $^{45}Ca^{2+}$ due to Ca^{2+} exchange with site II (42-44, see supplemental Figure S1). Then, $^{45}Ca^{2+}$ uptake assay in a single turnover was performed as in Fig. 4. In *A*, the time course obtained with the ADP-chase was best described by a single-exponential Ca^{2+} uptake (*solid line*) with a rate constant of 0.45 s^{-1} and maximum Ca^{2+}/*E*P value of 0.75. In *B*, it was best described by a double-exponential increase (*broken line*) with a rate constant and maximum value of 6.0 s^{-1} and 0.34 for the fast phase and 0.41 s^{-1} and 0.56 for the slow phase (but not described by a single-exponential increase shown as *solid line* with the rate constant 1.36 s^{-1} and the maximum value of 0.80).

FIGURE 6. Ca^{2+} dependence of *E*1P accumulation and Ca^{2+} binding in steady state. *A*, SR vesicles (200 μg/ml) were phosphorylated at 4 ºC for 30 s with 100 μM [γ-^{32}P]ATP in 3 μM A23187, 0.1 M LiCl, and 20 μM $CaCl_2$ with various concentrations of EGTA to give the indicated free Ca^{2+} concentrations. The total amount of *E*P (*closed circles*) and amount of *E*1P (*open circles*) were determined as in Fig. 3. *Solid lines* show the least squares fit to the Hill equation. The maximum, $K_{0.5}$, and Hill coefficient for the total amount of *E*P were 3.67 nmol/mg, 0.10 μM, and 2.6, respectively, and those for *E*1P were 2.12 nmol/mg, 0.11 μM, and 2.5, respectively. *B*, SR vesicles were phosphorylated with 100 μM ATP (*open squares*) or incubated without ATP (*closed squares* and *open triangles*) in 20 μM $^{45}CaCl_2$ with various concentrations of EGTA and 0.1 M LiCl (*squares*) or KCl (*triangles*), otherwise as in *A*. Then, 50 μl of the reaction mixture was spotted on the membrane, and the amount of $^{45}Ca^{2+}$ specifically bound to the ATPase was determined. *Solid lines* show the least squares fit to the Hill equation. The maximum, $K_{0.5}$, and Hill coefficient were 8.54 nmol/mg, 0.18 μM and 2.1 (*open triangles*), 7.82 nmol/mg, 0.20 μM, and 2.3 (*closed squares*), and 4.14 nmol/mg, 0.15 μM, and 1.5 (*open squares*). *C*, the amount of *E*1P (*open circles*) in *A* and that of bound $^{45}Ca^{2+}$ under the phosphorylating condition (*open squares*) in *B* in the absence of K^+ are replotted after normalization to the maximum total amount of *E*P and to the maximum $^{45}Ca^{2+}$ binding under the non-phosphorylating condition (*E*1) in the absence of K^+, respectively, and shown as % values. *Solid lines* show the least squares fit to the Hill equation and the maximum values were 58% for *E*1P and 52% for bound $^{45}Ca^{2+}$, respectively.

FIGURE 7. Schematic model for roles of K^+ in *E*P-processing and Ca^{2+}-handling in Ca^{2+} transport. "s*E*1PCa_2" is an *E*1PCa_2 species formed without K^+ possessing a closed cytoplasmic gate and lumen-facing Ca^{2+} binding sites (an opened lumenal pathway) with high Ca^{2+} affinity (Fig. 6). s*E*1PCa_2 is in rapid equilibrium with the normal *E*1PCa_2. Here, "s" denotes silent because this species is apparently absent in the presence of K^+, and also because the bound Ca^{2+} ions are not released to the cytoplasmic side even upon ADP-induced reverse dephosphorylation (to s*E*1Ca_2) in contrast to the normal *E*1PCa_2 reverse dephosphorylation. Actual active Ca^{2+} transport is achieved by a large reduction of the Ca^{2+} affinity during the normal sequence *E*1PCa_2 → *E*2PCa_2 → *E*2P + 2Ca^{2+} (*blue arrows*). The cartoon is based on crystal structural models for the ADP-sensitive and -insensitive *E*P states and *E*1Ca_2, with the positions of the cytoplasmic N, P, and A domains, and membrane (*orange layer*) being approximate. The Ca^{2+} sites in the transmembrane domain are depicted as occluded (closed cytoplasmic and lumenal gates) in normal *E*1PCa_2, as lumen-facing and high Ca^{2+} affinity with the closed cytoplasmic gate in s*E*1PCa_2 and s*E*1Ca_2, and as lumenally opened with reduced Ca^{2+} affinity in *E*2P and *E*2PCa_2 (immediately before the Ca^{2+} release).

FIGURE 8. Structure of *E*1PCa$_2$ with bound K$^+$. The crystal structure *E*1PCa$_2$·AMPPN (PDB code 3BA6) (22) is shown. *Panel a*, a space-filling model with K$^+$ (*blue*), M3 (*yellow*), M4 (*orange*), L6-7 (*lime*), Pα1 (*pink*), Pα6/Pα7 (*ice blue*), Glu^{732} (*red* and *cyan*), and A/M3-linker (*dark gray*). *Panel b*, a cartoon model with the view from the same direction as in *panel a*. K$^+$ and Ca^{2+} are *blue* and *red* Van der Waals spheres, respectively. M3, M4 and M5 are *yellow*, *orange* and *ice blue*, respectively. The lower panels in *a* and *b* are the enlarged view of the areas surrounded by *red broken line*. In *b*, the coordination of K$^+$ is shown by *broken green lines*. *Panel c*, the helices for Ca^{2+} binding (M4, M5, M6, and M8) and K$^+$ binding (Pα6/Pα7), and adjacent components (M3, M7, Pα1, and A/M3-linker) are depicted. A large *red arrow* suggests a possible motion of M3/M4L at the lumenal end to open the Ca^{2+} pathway. The residues involved in coordination of K$^+$ and Ca^{2+} are depicted in ball and stick representation. Residues possibly forming interactions at the lumenal end (Tyr^{294}, Tyr^{295}, Lys^{297}, and Glu^{785}) are also depicted. The *lower panel* in *c* shows the view from lumenal side.

FIGURE 9. Structural change during *E*1PCa$_2$ → *E*2P + 2Ca^{2+} and movement of the K$^+$-binding site. The structural change is modeled on the crystal structures with bound K$^+$, *E*1PCa$_2$·AMPPN and *E*2·AlF$_4^-$ (PDB code, 3BA6 (22) and 1XP5, (20) respectively). The two structures are aligned with the static M8-M10 helices. The approximate position of the transmembrane region (TM) is shown by *green lines*. The area indicated by *red dashed lines* in the whole molecule is enlarged in the *lower panel*. The motions of each of N, P, and A domains during *E*1PCa$_2$·AMPPN → *E*2·AlF$_4^-$ are indicated by *curved arrows*. Note that the K$^+$ site with bound K$^+$ on the P domain moves down to the Gln^{244} region on the A/M3-linker (*blue arrow*), thus likely cross-linking the P domain with the A/M3-linker. There are three critical interaction networks to realize and stabilize the compactly organized *E*2P structure. They are Tyr^{122}-HC forming a hydrophobic interaction cluster (*violet Van der Waals spheres*), the Val^{200}-loop (*red loop*), and TGES^{184} (*blue loop*) (10-13). Crystal structures of *E*2·BeF$_3^-$ (21, 22) which are analogs of the *E*2P ground state (25) are not used here because they were formed without K$^+$ (although the above noted changes are also seen with the *E*2·BeF$_3^-$ crystals).

SUPPLEMENTAL MATERIAL

for the manuscript by

Kazuo Yamasaki, Takashi Daiho, Stefania Danko, and Hiroshi Suzuki

Ca^{2+} Release to Lumen from ADP-sensitive Phosphoenzyme *E*1PCa_2 without Bound K^+ of Sarcoplasmic Reticulum Ca^{2+}-ATPase

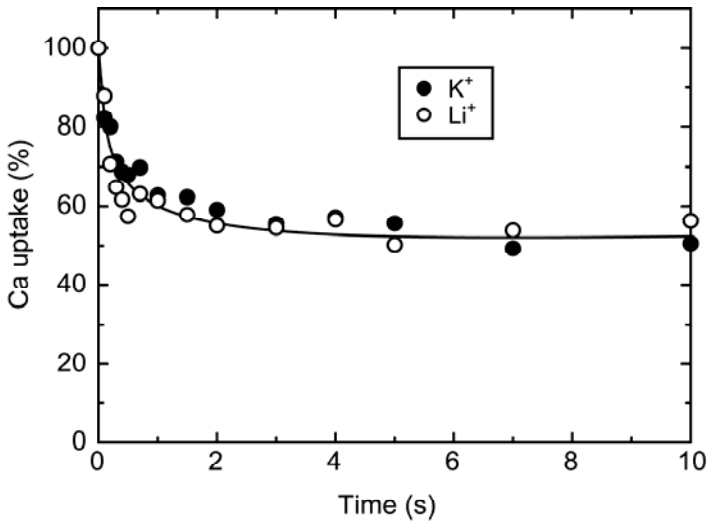

Supplemental Figure S1.
Labeling Site I by $^{45}Ca^{2+}$.
SR vesicles (20 μg/ml) were incubated with 10 μM $^{45}CaCl_2$ for ~10 min, then diluted by an equal volume of a solution containing 2 mM non-radioactive $CaCl_2$. After the subsequent incubation for the indicated time periods, Ca^{2+} uptake in a single turnover of *E*P was initiated by mixing with an equal volume of a solution containing 20 μM ATP and 2 mM EGTA. Immediately, the sample was spotted on the membrane filter and washed for ~10 s by the EGTA solution as in Fig. 4, and the amount of $^{45}Ca^{2+}$ uptake was determined. All the solutions contained 0.1 M KCl (*closed circles*) or LiCl (*open circles*).

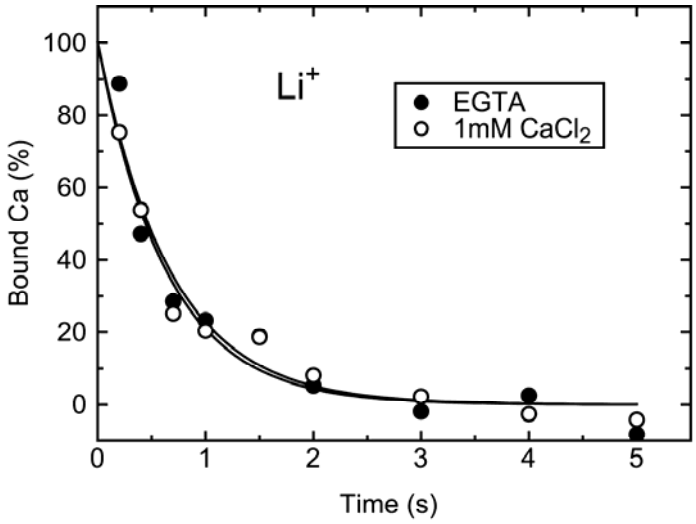

Supplemental Figure S2.
Non-sequential $^{45}Ca^{2+}$ release from E1PCa$_2$ without K^+. SR vesicles (20 μg/ml) were phosphorylated for 30 s with 10 μM ATP in 10 μM $^{45}CaCl_2$, 3 μM A23187, and 0.1 M LiCl. Then an aliquot of the solution was spotted on the membrane and washed by a washer containing 0.1 M LiCl, 3 μM A23187, and non-radioactive 1 mM $CaCl_2$ (*open circles*) or 2 mM EGTA (*closed circles*) for the indicated time periods. The amounts of $^{45}Ca^{2+}$ specifically bound to the Ca^{2+}-ATPase were determined. *Solid lines* show the least squares fit to a single-exponential.

Note, if the Ca^{2+} release is sequential, the biphasic $^{45}Ca^{2+}$ release would take place when the first released $^{45}Ca^{2+}$ is exchanged by non-radioactive 1 mM Ca^{2+} (which is high enough for binding to the Ca^{2+} sites (Fig 6). We found the same single-exponential $^{45}Ca^{2+}$ release kinetics upon the addition of excess EGTA and that of 1 mM Ca^{2+}. The results show that the Ca^{2+} release from *E*1PCa$_2$ in the absence of K^+ is non-sequential, as previously observed in the presence of K^+ for the normal release process *E*1PCa$_2$ → *E*2PCa$_2$ → *E*2P + 2Ca^{2+} (58, 59).

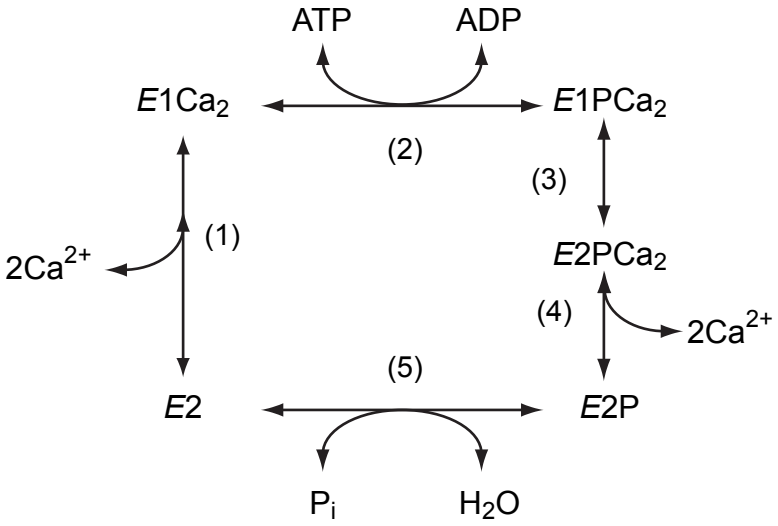

Figure 1

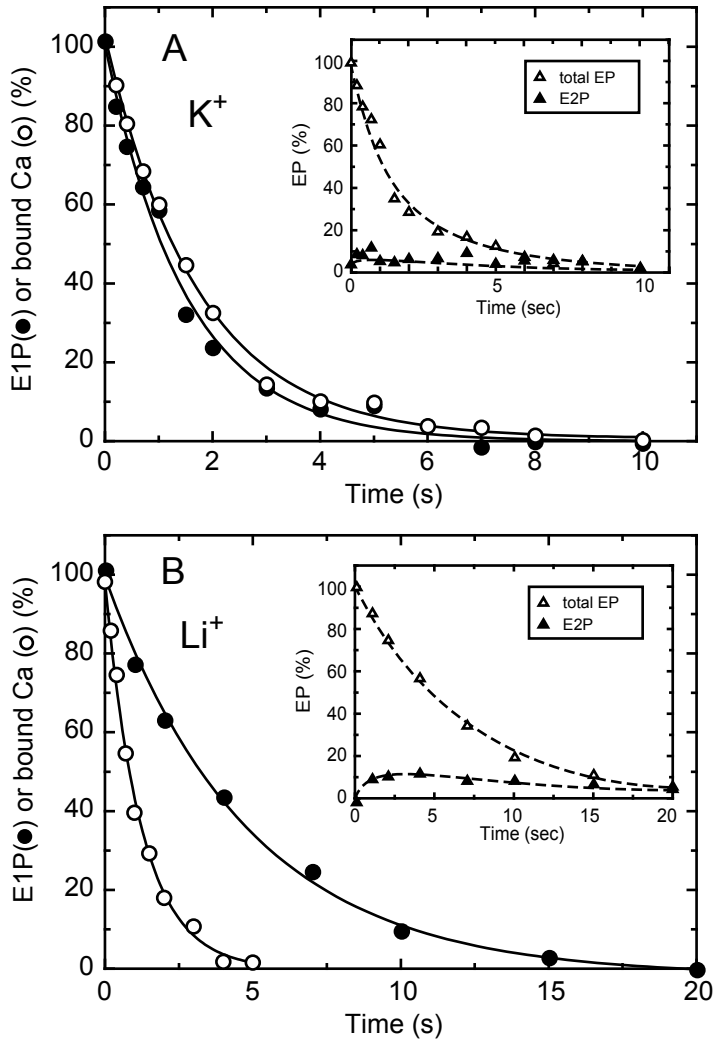
A
K+
E1P(●) or bound Ca (o) (%)
Time (s)
total EP
E2P
EP (%)
Time (sec)
B
Li+
E1P(●) or bound Ca (o) (%)
Time (s)
total EP
E2P
EP (%)
Time (sec)

Figure 2

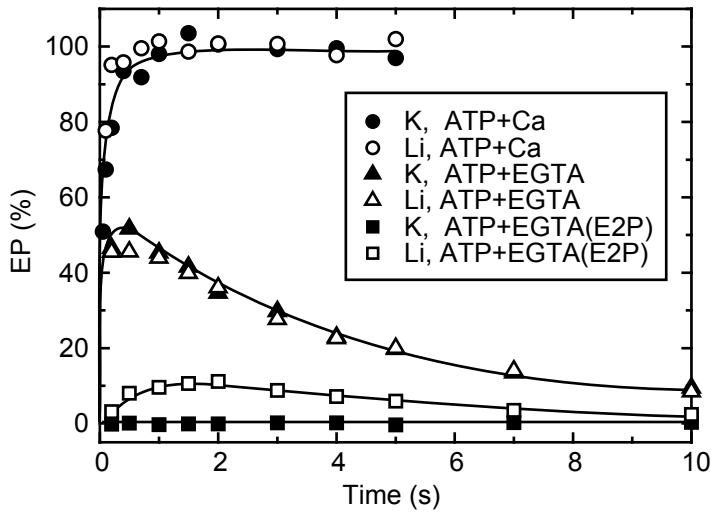
EP (%)
Time (s)
K, ATP+Ca
Li, ATP+Ca
K, ATP+EGTA
Li, ATP+EGTA
K, ATP+EGTA(E2P)
Li, ATP+EGTA(E2P)

Figure 3

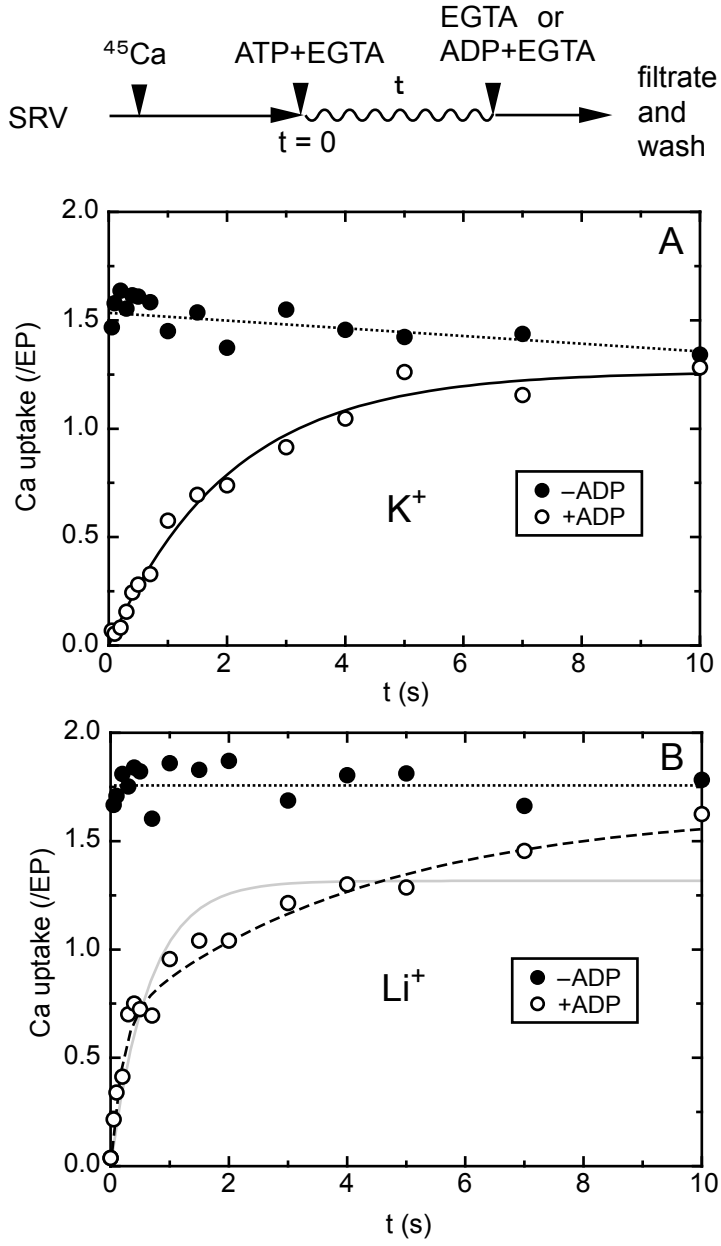
45Ca
ATP+EGTA
EGTA or
ADP+EGTA
t
SRV
t = 0
filtrate
and
wash
A
Ca uptake (/EP)
K+
–ADP
+ADP
t (s)
B
Li+
–ADP
+ADP
t (s)

Figure 4

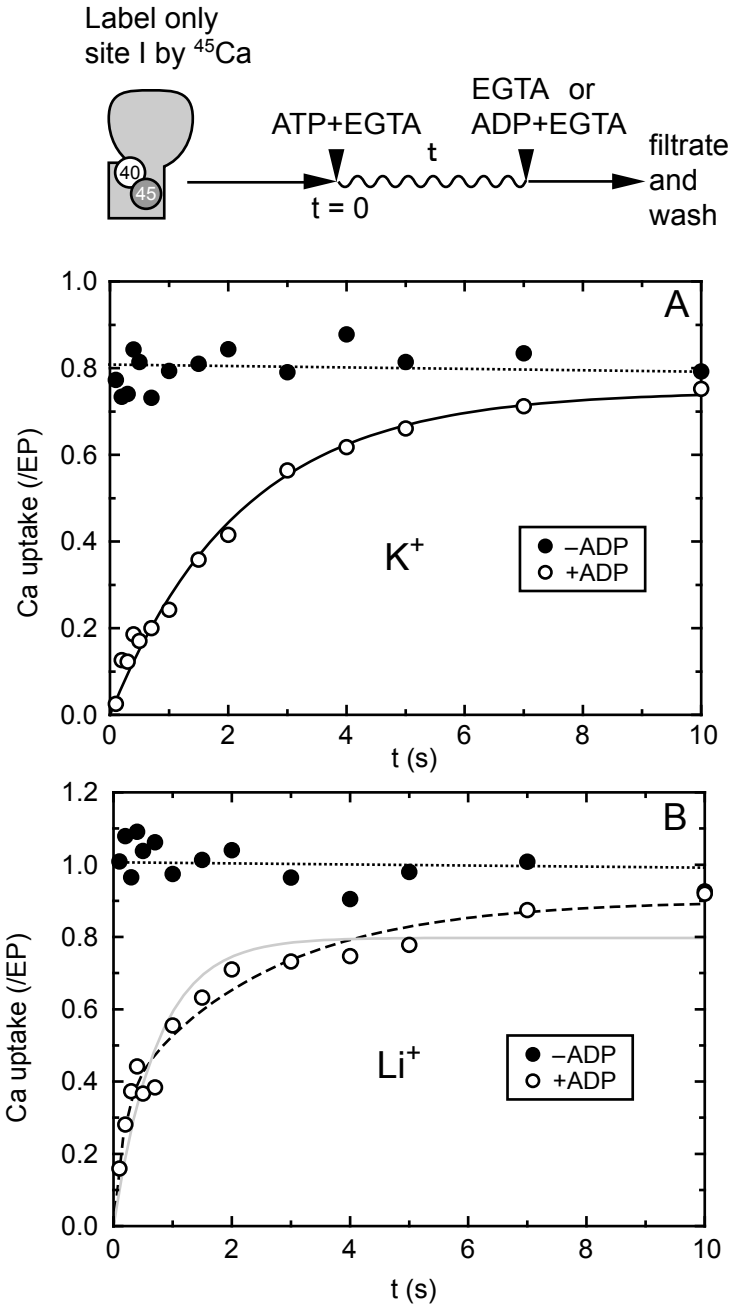
Label only
site I by 45Ca
ATP+EGTA
t
EGTA or
ADP+EGTA
filtrate
and
wash
t = 0
40
45
A
K+
–ADP
+ADP
Ca uptake (/EP)
t (s)
B
Li+
–ADP
+ADP
Ca uptake (/EP)
t (s)

Figure 5

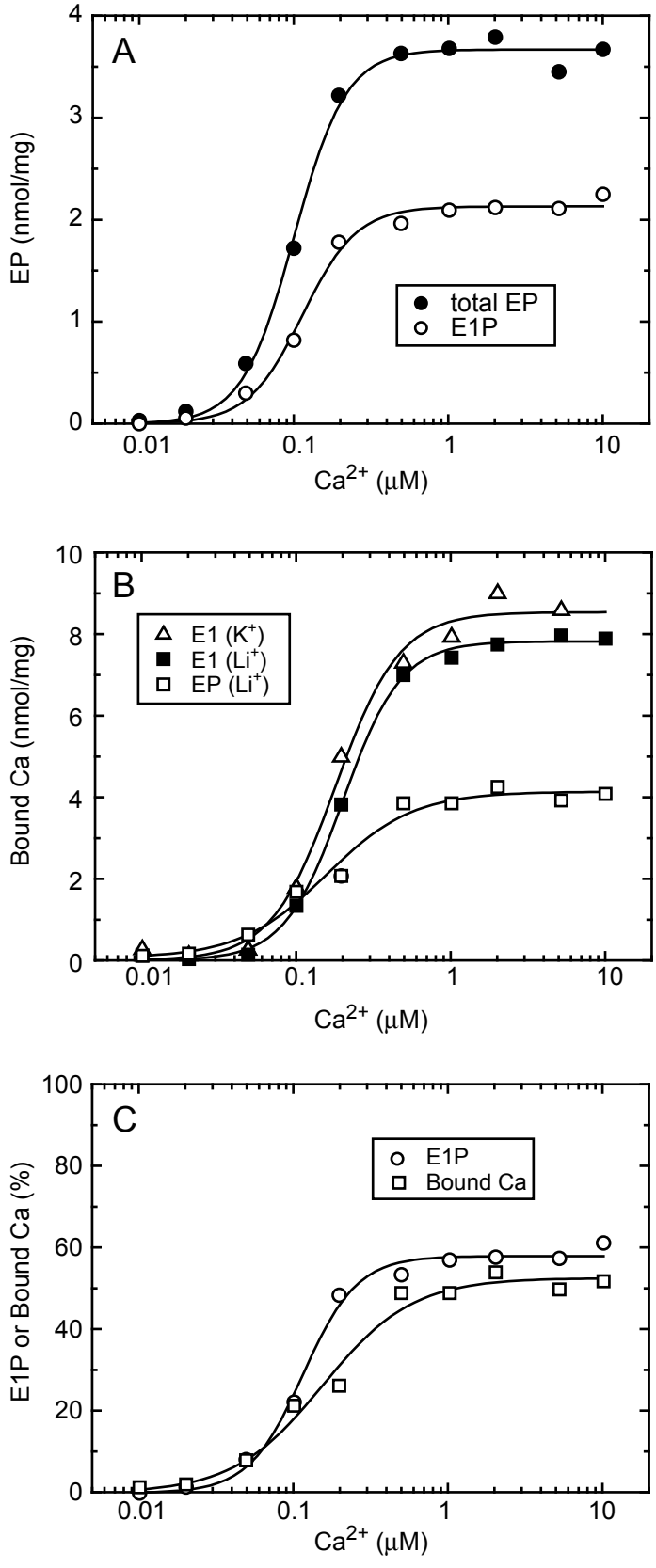
A
EP (nmol/mg)
total EP
E1P
Ca2+ (μM)
B
Bound Ca (nmol/mg)
E1 (K+)
E1 (Li+)
EP (Li+)
Ca2+ (μM)
C
E1P or Bound Ca (%)
E1P
Bound Ca
Ca2+ (μM)

Figure 6

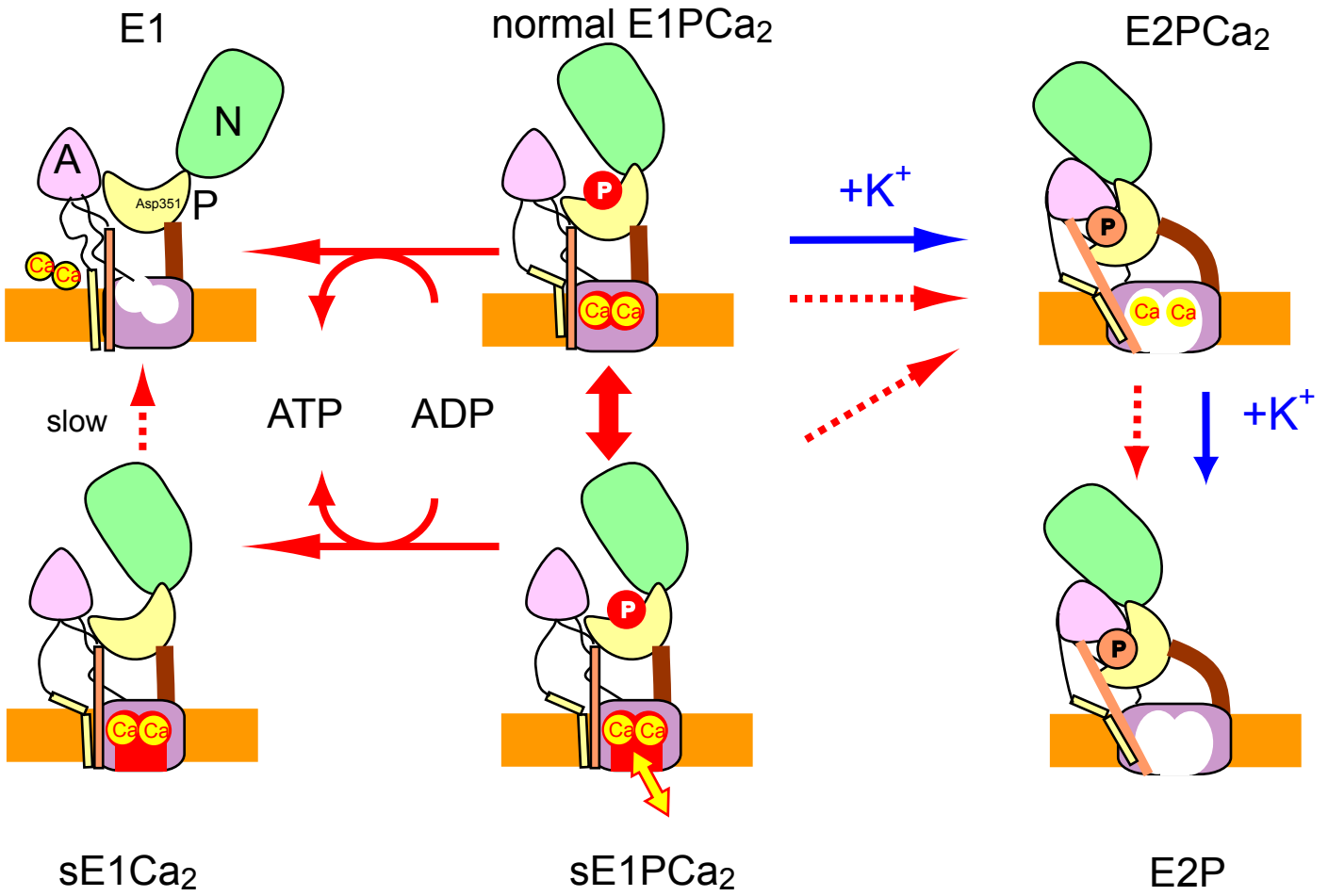
E1
normal E1PCa2
E2PCa2
N
A
Asp351
P
Ca
Ca
P
+K+
slow
ATP
ADP
+K+
sE1Ca2
sE1PCa2
E2P

Figure 7

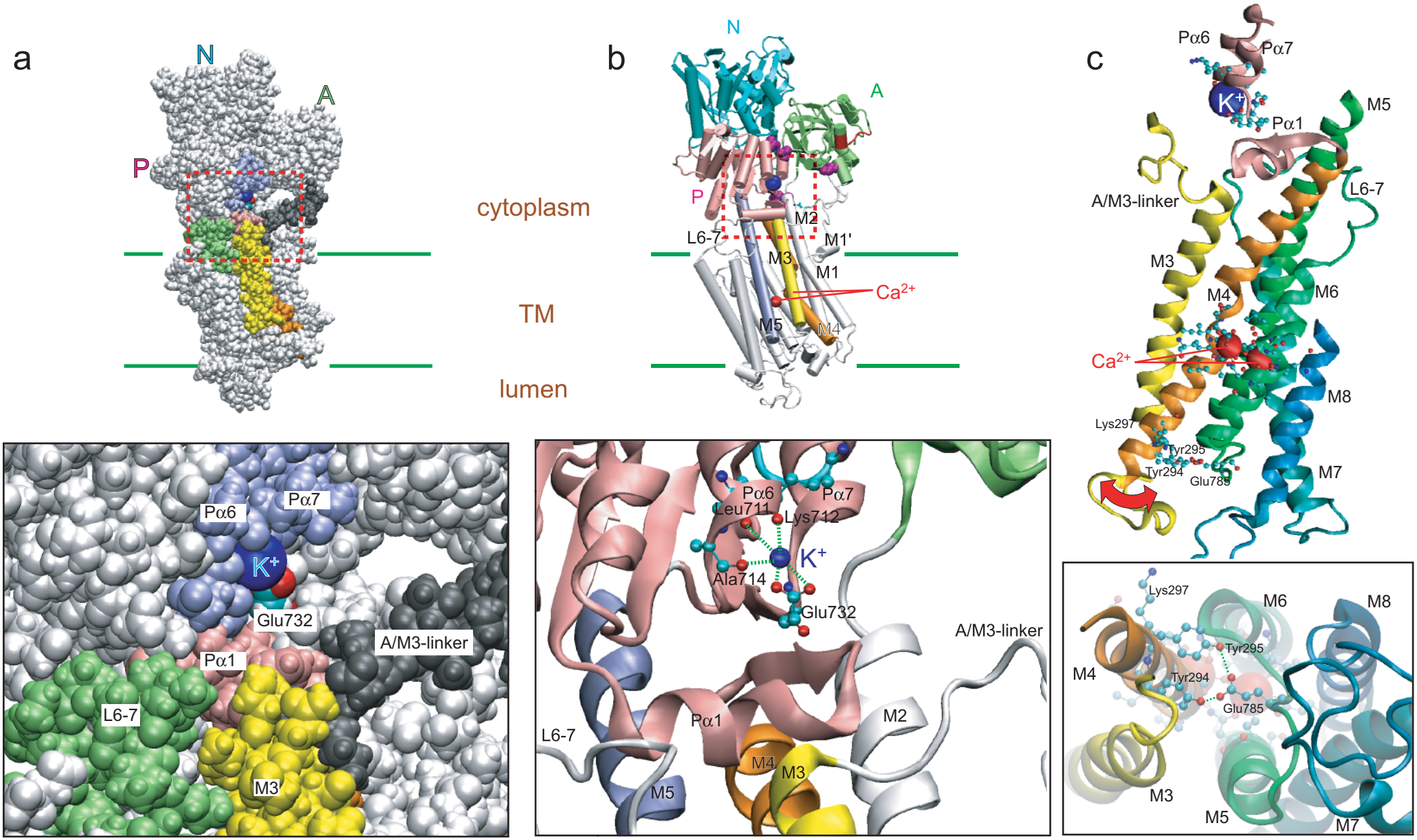
a
N
A
P
cytoplasm
TM
lumen
b
N
A
P
M2
L6-7
M1'
M3
M1
Ca2+
M5
M4
c
Pα6
Pα7
K+
M5
Pα1
L6-7
A/M3-linker
M3
M4
M6
Ca2+
M8
Lys297
Tyr295
Tyr294
Glu785
M7
Pα6
Pα7
K+
Glu732
A/M3-linker
Pα1
L6-7
M3
Pα6
Pα7
Leu711
Lys712
K+
Ala714
Glu732
A/M3-linker
L6-7
Pα1
M2
M4
M3
M5
Lys297
M6
M8
Tyr295
M4
Tyr294
Glu785
M3
M5
M7

Figure 8

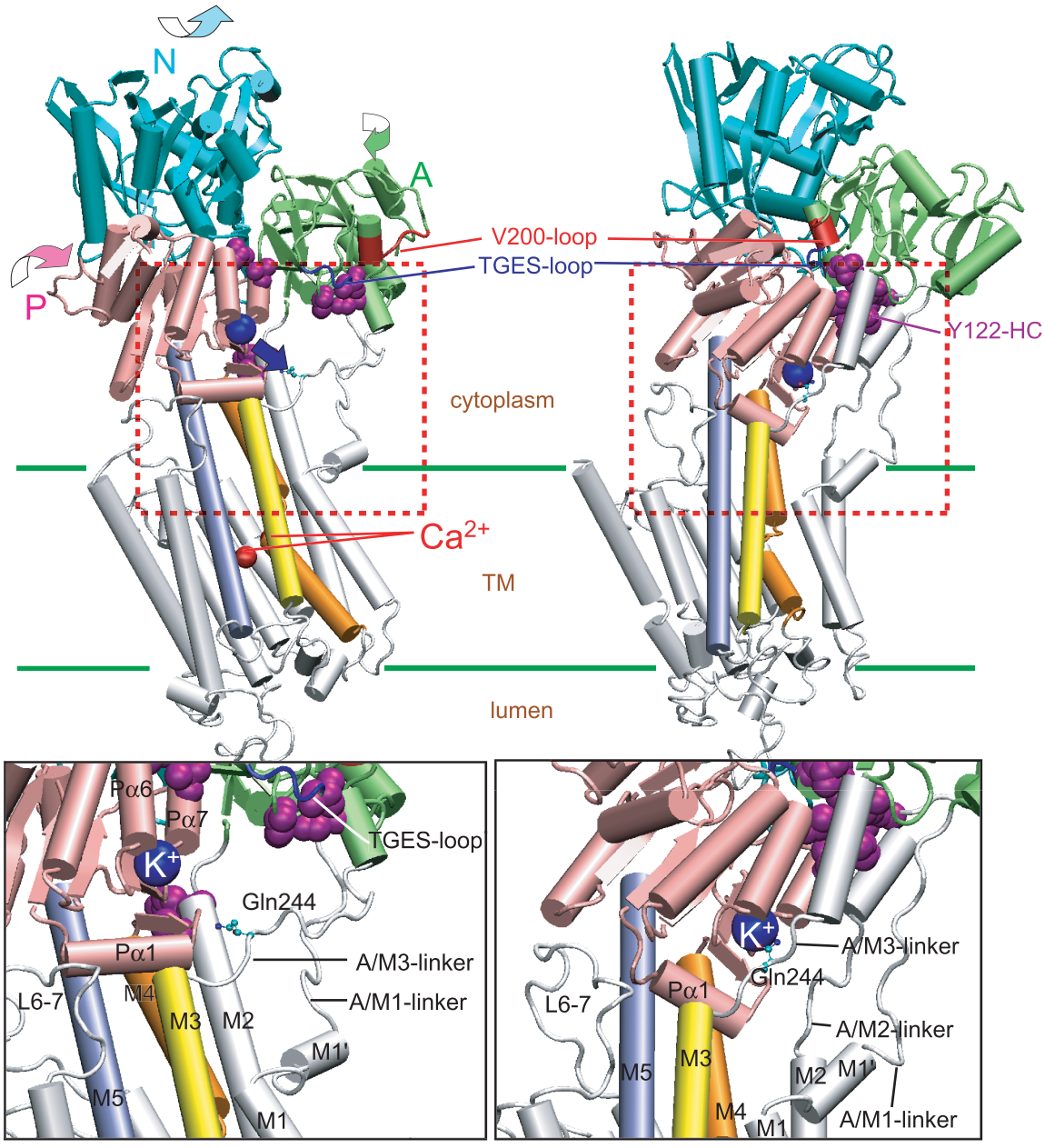

E1PCa$_2$ /AMPPN (3BA6)

E2·AlF$_4^-$(TG) (1XP5)

Figure 9

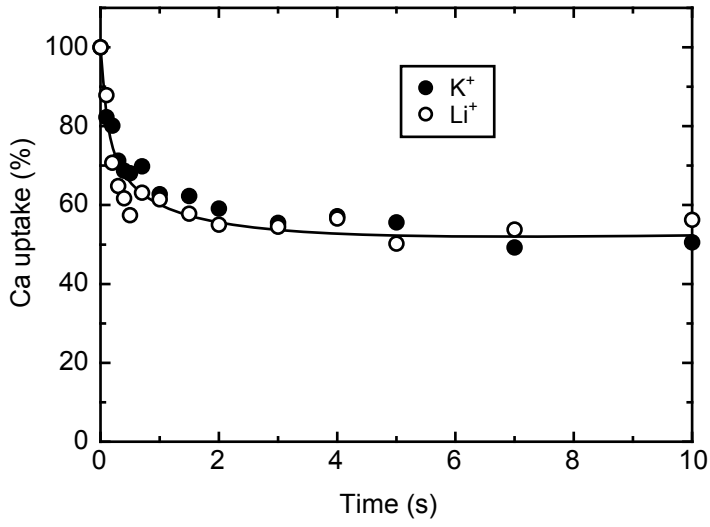

Supplemental Figure S1

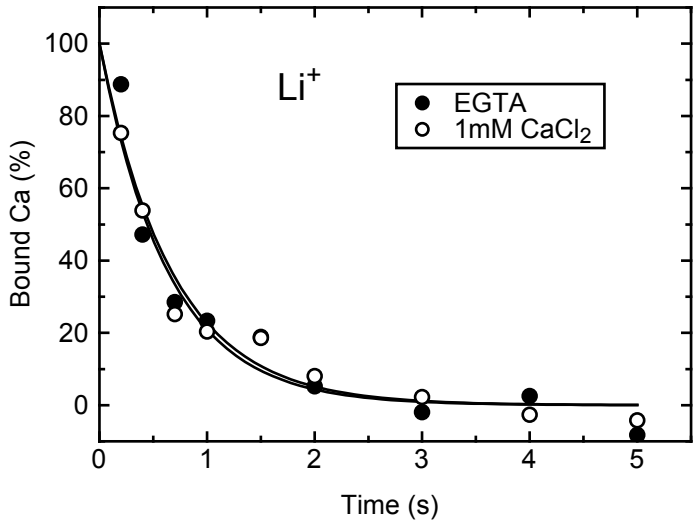

Supplemental Figure S2